Journal of Applied Sciences

ISSN 1812-5654

science alert

ANSInet
an open access publisher
http://ansinet.com

Journal of Applied Sciences 9 (6): 1128-1134, 2009
ISSN 1812-5654

Effects of Air-Fuel Ratio and Engine Speed on Performance of Hydrogen Fueled Port Injection Engine

M.M. Rahman, Mohammed K. Mohammed and Rosli A. Bakar
Automotive Excellence Center, Faculty of Mechanical Engineering,
Universiti Malaysia Pahang, Locked Bag 12, 25000 Kuantan, Pahang, Malaysia

Abstract: This study was investigated the effect of air-fuel ratio (AFR) and engine speed on performance of the single cylinder hydrogen fueled port injection engine. GT-Power was utilized to develop the computational model for port injection engine. One dimensional gas dynamics model was represented the flow and heat transfer in the components of the engine. Throughout the study, air-fuel ratio was varied from stoichiometric mixture to lean. The engine speeds were varied from 2500 to 4500 rpm. The results show that the air-fuel ratio and engine speed were greatly influence on the performance of hydrogen fueled engine especially Brake Mean Effective Pressure (BMEP), thermal efficiency and brake specific fuel consumption (BSFC). It was shown that decreases of the BMEP and brake thermal efficiency with increases of the engine speed and air-fuel ratio while the increases of the BSFC with increases of the speed and air-fuel ratio. The cylinder temperature increases with increases of engine speed however temperature decreases with increases of air-fuel ratio. The volumetric efficiency increases with increases of engine speed and equivalent ratio. The volumetric efficiency of the hydrogen engines with port injection is serious problem and reduces the overall performance of the engine. This emphasized the ability of retrofitting the traditional engines with hydrogen fuel with minor modifications.

Key words: Hydrogen fueled engine, port injection, air fuel ratio, engine speed, performance characteristics

INTRODUCTION

Energy is currently uppermost in everyone's minds. Recent price hikes for domestic gas and electricity, coupled with fluctuating oil prices, concerns about where our future energy will come from and the impact of energy use on climate change have all brought energy policy to the top of the political agenda. The alarming rise in pollution levels in the atmosphere and increased concern for energy independency are the two major driving factors for seeking alternative fuels. Among the viable options, hydrogen is the only non-carbonaceous fuel available on the earth. Therefore, hydrocarbon and carbon monoxide free engine operation with hydrogen. Hydrogen has been regarded as a future secondary fuel for power systems due to CO_2 and hydrocarbon free operation. Recent drastic increase in the price of petroleum, rapid increase in emission of green house gases and very strict environmental legislations are major motivating factors for usage of hydrogen in fuel cells and internal combustion engines. Hydrogen as a fuel for internal combustion engine is best suited for spark ignition due to its high self-ignition temperature (Ganesh *et al*., 2008). A lean mixture results in an improvement of fuel economy. More complete combustion, lower combustion temperature and reduced pollutants (COD, 2001). Normally, cycle by cycle variations occur in the engines operating with very lean mixtures. But, with hydrogen, these variations are much less compared to that of engines powered by other hydrocarbon fuels (Kim *et al*., 2005). Hydrogen needs very low ignition energy, which ensures prompt ignition. Hydrogen induction techniques play a very dominant and sensitive role in determining the performance characteristics of the hydrogen fueled internal combustion engine (Suwanchotchoung, 2003). Hydrogen fuel delivery system can be broken down into three main types including the carbureted injection, port injection and direct injection (COD, 2001).

The port injection fuel delivery system injects hydrogen directly into the intake manifold at each intake port rather than drawing fuel in at a central point. Typically, hydrogen is injected into the manifold after the beginning of the intake stroke (COD, 2001). Hydrogen can be introduced in the intake manifold either by continuous or timed injection. The former method produces

Corresponding Author: M.M. Rahman, Faculty of Mechanical Engineering, Universiti Malaysia Pahang, Locked Bag 12, 25000 Kuantan, Pahang, Malaysia Tel: +6-09-5492207 Fax: +6-09-5492244

undesirable combustion problems, less flexible and controllable (Das, 1990). But the latter method, timed port fuel injection (PFI) is a strong candidate and extensive studies indicated the ability of its adoption (Das *et al*., 2000; Das, 2002). This technique is supported by a considerable set of advantages. It can be easily installed with simple modification (Lee *et al*., 1995) and its cost is low (Li and Karim, 2006). The flow rate of hydrogen supplied can also be controlled conveniently (Sierens and Verhelst, 2001). External mixture formation by means of port fuel injection also has been demonstrated to result in higher engine efficiencies, extended lean operation, lower cyclic variation and lower NO_x production (Yi *et al*., 2000; Rottengruber *et al*., 2004; Kim *et al*., 2006). There are consequence of the higher mixture homogeneity due to longer mixing times for PFI. Furthermore, external mixture formation provides greater degree of freedom concerning storage methods (Verhelst *et al*., 2006). The most serious problem with PFI is the high possibility of pre-ignition and backfire, especially with rich mixtures (Kabat and Heffel, 2002; Ganesh *et al*., 2008). However, conditions with PFI are much less severe and the probability for abnormal combustion is reduced because due to it's imparts a better resistance to backfire (COD, 2001). Combustion anomalies can be suppressed by accurate control of injection timing and elimination of hot spots on the surface of the combustion as suggested by Lee *et al*. (1995). The present study is developed the computational model for a single cylinder, port injection hydrogen fueled internal combustion engine. The objective of this study is to investigate the effect of air fuel ratio and engine speed on the performance characteristics of this engine.

MATERIALS AND METHODS

Engine performance parameters: The brake mean effective pressure (BMEP) can be defined as the ratio of the brake work per cycle W_b to the cylinder volume displaced per cycle V_d and it can be expressed as in Eq. 1:

$$BMEP = \frac{W_b}{V_d} \quad (1)$$

Equation 1 can be rewrite for the four stroke engine as in Eq. 2:

$$BMEP = \frac{2P_b}{NV_d} \quad (2)$$

where, P_b is the brake power and N is the engine speed.

Brake efficiency (η_b) can be defined as the ratio of the brake power to the engine fuel energy which is expressed as in Eq. 3:

$$\eta_b = \frac{P_b}{\dot{m}_f (LHV)} \quad (3)$$

where, $\dot{m}_f$ is the fuel mass flow rate and LHV is the lower heating value of hydrogen.

The brake specific fuel consumption (BSFC) represents the fuel flow rate per unit brake power output and can be expressed as in Eq. 4:

$$BSFC = \frac{\dot{m}_f}{P_b} \quad (4)$$

The volumetric efficiency (η_v) of the engine is defines as the mass of air supplied through the intake valve during the intake period ($\dot{m}_a$) by comparison with a reference mass, that mass required to perfectly fill the swept volume under the atmospheric conditions. It can be expressed as in Eq. 5:

$$\eta_v = \frac{\dot{m}_a}{\rho_{ai} V_d} \quad (5)$$

where, ρ_{ai} is the inlet air density.

Engine model: A single cylinder, four stroke, port injection hydrogen fueled engine was modeled utilizing the GT-Power software. The injection of hydrogen was located in the midway of the intake port. The model of the hydrogen fueled single cylinder four stroke port inject engine is shown in Fig. 1. Engine specifications for the base engine are shown in Table 1. The specific values of input parameters including the AFR, engine speed and injection timing were defined in the model. The boundary condition of the intake air was defined first in the entrance of the engine. The air enters through a bell-mouth orifice to the pipe. The discharge coefficients of the bell-mouth orifice were set to 1 to ensure the smooth transition as in the real engine. The pipe of bell-mouth orifice with 0.07 m of diameter and 0.1 m of length are used in this model. The pipe connects in the intake to the air cleaner with 0.16 m of diameter and 0.25 m of length was modeled. The air cleaner pipe identical to the bell-mouth orifice connects to

Table 1: Hydrogen fueled engine parameters

Engine parameters (unit)	Value
Bore (mm)	100
Stroke (mm)	100
Connecting rod length (mm)	220
Piston pin offset (mm)	1.00
Displacement (cm^3)	3142
Compression ratio	9.5
Inlet valve close IVC (°CA)	-96
Exhaust valve open EVO (°CA)	125
Inlet valve open IVO (°CA)	351
Exhaust valve close EVC (°CA)	398

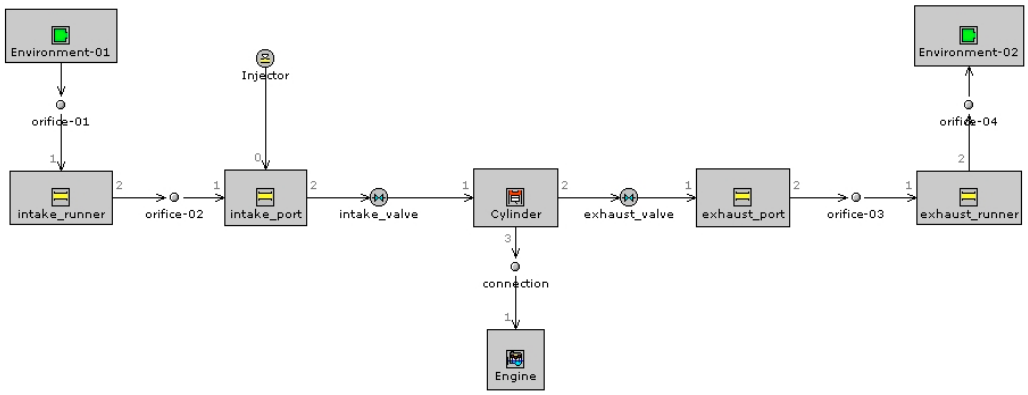

Fig. 1: Model of single cylinder, four stroke, port injection hydrogen fueled engine

the manifold. A log style manifold was developed from a series of pipes and flow-splits. Firstly, an attribute heat transfer multiplier is used to account for bends, roughness and additional surface area and turbulence caused by the valve and stem. Also, the pressure losses in these ports are included in the discharge coefficients calculated for the valves. The total volume for each flow-split was 256 cm^3. The flow-splits compose from an intake and two discharges. The intake draws air from the preceding flow-split. One discharge supplies air to adjacent intake runner and the other supplies air to the next flow-split. The last discharge pipe was closed with a cup to prevent any flow through it because there is no more flow-split. The flow-splits are connected with each other via., pipes with 0.09 m diameter and 0.92 m length. The junctions between the flow-splits and the intake runners were modeled with bell-mouth orifices. The discharge coefficients were also set to 1 to assure smooth transition, because in most manifolds the transition from the manifold to the runners is very smooth. The intake runners for the four cylinders were modeled as four identical pipes with 0.04 m diameter and 0.1 m length. Finally the intake runners were linked to the intake ports which were modeled as pipes with 0.04 m diameter and 0.08 length. The air mass flow rate in the intake port was used for hydrogen flow rate based on the imposed AFR.

The in-cylinder heat transfer is calculated by a formula which closely emulates the classical Woschni correlation. Based on this correlation, the heat transfer coefficient (h_c) can be expresses as in Eq. 6:

$$h_c = 3.26B^{-0.2}p^{0.8}T^{-0.55}w^{0.8} \quad (6)$$

where, B is the bore in meters, p is the pressure in kPa, T is temperature in K and w is the average cylinder gas velocity in m sec^{-1}.

Table 2: Temperature of the mail engine parts

Components	Temperature (K)
Cylinder head	550
Cylinder block wall	450
Piston	590

Table 3: Parameters used in the exhaust environment

Parameters	Value	Unit
External environment temperature	320	K
Heat transfer coefficient	15	W/m^2 K
Radiation temperature	320	K
Wall layer material	Steel	
Layer thickness	3	mm
Emissivity	0.8	

The combustion burn rate (X_b) using Wiebe function, can be expressed as in Eq. 7:

$$X_b = 1 - \exp\left[-a\left(\frac{\theta - \theta_i}{\Delta\theta}\right)^{n+1}\right] \quad (7)$$

where, θ is the crank angle, θ_i is the start of combustion, $\Delta\theta$ the combustion period and a and n are adjustable parameters. The overall temperature of the head, piston and cylinder for the engine parts are shown in Table 2. The temperature of the piston is higher than the cylinder head and cylinder block wall temperature because this part is not directly cooled by the cooling liquid or oil. Exhaust system walls temperature was calculated using a model embodied in each pipe and flow-split. Table 3 shown the parameters used in the exhaust environment of the model.

RESULTS AND DISCUSSION

It is worthy to mention that one of the most attractive combustive features for hydrogen fuel, which is its wide range of flammability. A lean mixture is the amount of fuel less than stoichiometric mixture. This leads to fairly easy to obtain an engine start. In the present model, hydrogen was injected into the cylinder within a timing range started

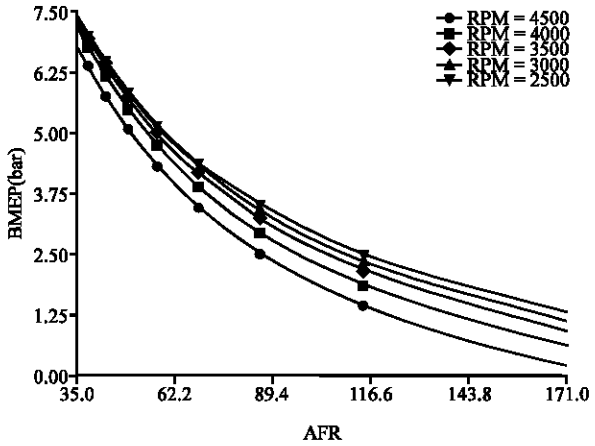

Fig. 2: Variation of brake mean effective pressure with air fuel ratio for various engine speeds

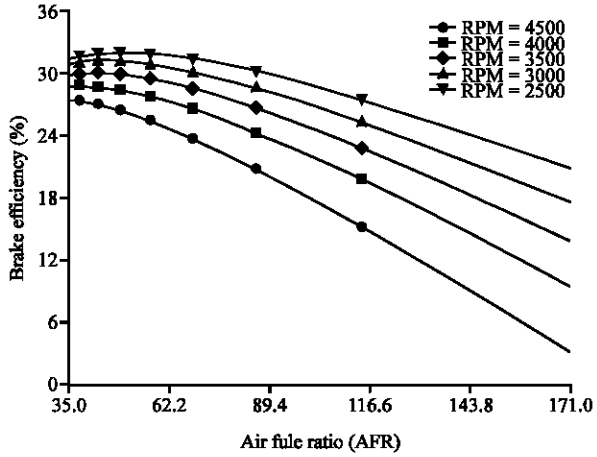

Fig. 3: Variation of brake thermal efficiency with air fuel ratio

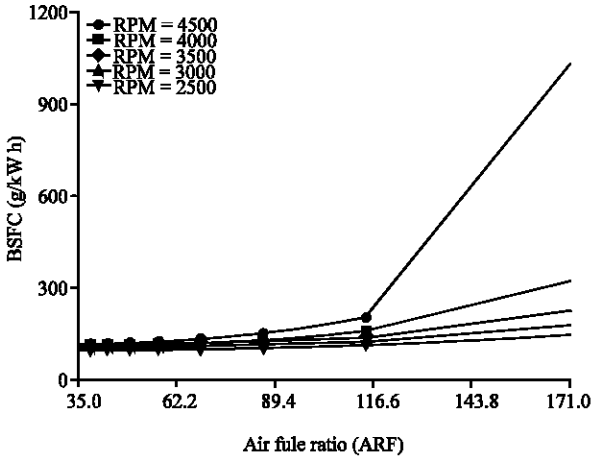

Fig. 4: Variation of brake specific fuel consumption with air fuel ratio for different engine speed

just before IVC (-96^0 BDC) until TDC (0^0). The air-fuel ratio was varied from stoichiometric limit (AFR = 34.33:1 based on mass where the equivalence ratio $\varphi = 1$) to a very lean limit (AFR =171.65 based on $\varphi = 0.2$) and engine speed varied from 2500 to 4500 rpm. Amount of hydrogen injected in one cycle is approximately 22 mg cycle^{-1} with injection pulse duration of 4.4 m sec.

Figure 2 shows the effect of air-fuel ratio on the brake mean effective pressure. BMEP is the good parameter for comparing engines with regard to design due to its independent on the engine size and speed. The large engine was always seem to be better when consider the torque, however, speeds become very important when consider the power (Pulkrabek, 2003). It is obtained from the results that the decreases of the BMEP with increases of AFR and speed. It is obvious that the BMEP falls with a non-linear behavior from the rich condition where AFR is 34.33 to the lean condition where the AFR is 171.65. The difference of BMEP increases with increases of speed and AFR. The differences of the BMEP are decrease of 6.682 bar at speed of 4500 rpm while 6.12 bar at speed 2500 rpm for the same range of AFR. This implied that the engine gives the maximum power (BMEP = 1.275 bar at lower speed 2500 rpm) compared with the power (BMEP = 0.18 bar) at speed 4500 rpm. Due to dissociation at high temperature combustion, molecular oxygen is present in the burned gases under stoichiometric conditions. Thus some additional fuel is added and partially burned. This increases the temperature and the number of moles of the burned gases in the cylinder. These effects increase the pressure; those were given increase power and mean effective pressure (Heywood, 1988).

Figure 3 shows the variation of the brake thermal efficiency with the air fuel ratio for the selected speeds. The brake power as a percentage is considered for the intake fuel energy and the fuel energy are covered the friction losses and heat losses (heat loss to surroundings, exhaust enthalpy and coolant load). It can be observed that the brake thermal efficiency increases nearby the richest condition (AFR $\cong$ 35) and then decreases with increases of AFR and speed. The operation within the range of AFR from 49.0428 to 42.91250 ($\varphi = 0.7$ to 0.8) give the maximum values for η_b for all speeds. Maximum η_b can be seen of 31.8% at speed 2500 rpm compared with 26.8% at speed 4500 rpm. Unaccepted η_b is observed of 2.88% at very lean conditions with AFR of 171.65 ($\varphi = 0.2$) for speed of 4500 rpm while 20.7% at the same conditions with speed of 2500 rpm. Clearly, engine rotational speed has a major effect in the behavior of η_b with AFR due to higher speeds lead to higher friction losses.

Figure 4 depicts the behavior of the brake specific fuel consumption with AFR. The AFR for optimum fuel consumption at a given load depends on the details

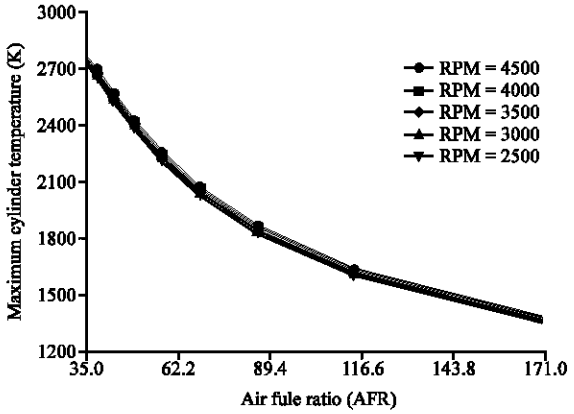

Fig. 5: Variation of maximum cylinder temperature with air fuel ratio

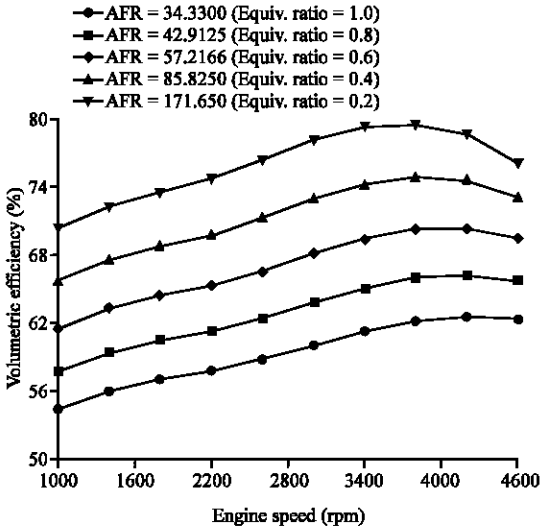

Fig. 6: Effect of volumetric efficiency with the rotational speed for different equivalence ratio

of chamber design including compression ratio and mixture preparation quality. It varies for a given chamber with the part of throttle load and speed range (Heywood, 1988). It is clearly seen from Fig. 4 that the higher fuel is consumed at higher speeds and AFR due to the greater friction losses that can occur at high speeds. It is easy to perceive from the figure that the increases of BSFC with decreases in the rotational speed and increases the value of AFR. However, the required minimum BSFC were occurred within the range of AFR from 38.144 (φ = 0.9) to 49.0428 (φ = 0.7) for the selected range of speed. At very lean conditions, higher fuel consumption can be noticed. After AFR of 114.433 (φ = 0.3) the BSFC increase rapidly, especially for high speed. At very lean conditions with AFR of 171.65 (φ = 0.2), the BSFC of 144.563 g kW^{-1} h was observed at 2500 rpm while 1038.85 g kW^{-1} h for speed of 4500 rpm. The value BSFC at speed 2500 rpm was observed around 2 times at 4000 rpm, however, around 7 times at 4500 rpm. This is because of very lean operation conditions, which can lead to unstable combustion and more lost power due to a reduction in the volumetric heating value of the air/hydrogen mixture. This behavior can be more clarified by Fig. 3, where the brake efficiency reduced considerably at very lean operation conditions.

Figure 5 shows the behavior AFR can affect the maximum temperature inside the cylinder. In general, lower temperatures are required due to the reduction of pollutants. It is clearly demonstrated that the decrease of maximum cylinder temperature with increases of AFR. The effect of the engine speed on maximum cylinder temperatures with AFR are not significant. At stoichiometric operating conditions (AFR = 34.33), the maximum cylinder temperature of 2752.83 K was recorded and it is dropped to 1350K at AFR of 171.65 (φ = 0.2). This lower temperature inhibits to the formation of NO_x pollutants. In fact this feature is one of the major motivations toward hydrogen fuel.

Figure 6 shows the variation of the volumetric efficiency with the engine speed. The volumetric efficient increase with increases of AFR. In general, it is desirable to have maximum volumetric efficiency for engine. The importance of volumetric efficiency is more critical for hydrogen engines because of the hydrogen fuel displaces large amount of the incoming air due to its low density (0.0824 kg m^{-3} at 25°C and 1 atm). This reduces the volumetric efficiency to high extent. The stoichiometric mixture of hydrogen and air consists of approximately 30% hydrogen by volume, whereas a stoichiometric mixture of fully vaporized gasoline and air consists of approximately 2% gasoline by volume (White, 2006). Therefore, the low volumetric efficiency for hydrogen engine is expected compared with gasoline engine works with the same operating conditions and physical dimension. This lower volumetric efficiency is apparent in Fig. 6. Leaner mixture gives the higher volumetric efficiency. The maximum volumetric efficiency was observed 79.4% at lean conditions with AFR = 171.65 (φ = 0.2) while 62.4% at stoichiometric conditions.

Higher speeds lead to higher volumetric efficiency because of the higher speeds give higher vacuum at the port and consequent larger air flow rate. Further increase in engine speed leads toward the maximum value of η_v. The volumetric efficiency increases with increases of engine at certain limit then decreases. For equivalences ratio until below 0.6, the maximum η_v was recorded at 4200 rpm. For equivalence ratio below 0.6, the

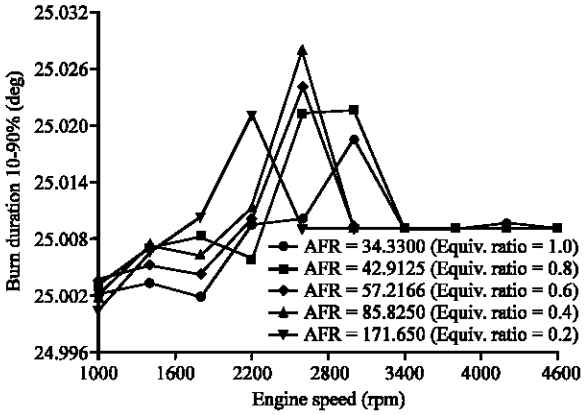

Fig. 7: Variation of combustion duration with engine speed for different equivalence ratio

maximum η_v was recorded at 3800 rpm. At further higher engine speeds beyond these values, the flow during at least part of the intake process becomes chocked. Once chocked occurs, further increase of speed does not increase the flow rate significantly, thus, the volumetric efficiency decreases sharply. This sharp decrease happens due to the charge heating in the manifold and higher friction flow losses. In fact that the several solution were suggested to solved this problem (Nagalingam *et al.*, 1983; Furuhama and Fukuma, 1986; Lynch, 1983) suggested and carried out tests with pressure boosting systems for hydrogen engine.

Figure 7 shows the combustion duration with the engine speed for different equivalence ratio. The hydrogen combustion velocity (1.85 m sec^{-1}) is rapid compared with that of gasoline (0.37-0.43 m sec^{-}). Therefore, the short combustion duration is expected. It is well established that the duration of combustion in crank angle (degree) increases slowly with increases of speed for gasoline and diesel engines (Heywood, 1988). This fact is also true for hydrogen engine (Fig. 7). The fluctuation shown in Fig. 7 is very small, however, it is enlarged in the Fig. 7 with a very high scale. The fluctuation take place within the range of 0.0248°CA.

CONCLUSION

The performance characteristics of single cylinder port injection hydrogen fueled engine were investigated. The following conclusions are drawn:

- At very lean conditions with low engine speeds, acceptable BMEP can be reached, while it is unacceptable for higher speeds. Lean operation leads to small values of BMEP compared with rich conditions
- Maximum brake thermal efficiency can be reached at mixture composition in the range of (φ = 0.7 to 0.9) and it decreases dramatically at leaner conditions.
- The desired minimum BSFC occurs within a mixture composition range of (φ = 0.7-0.9). The operation with very lean condition (φ<0.2) and high engine speeds (> 4500) consumes unacceptable amounts of fuel
- Lean operation conditions results in lower maximum cylinder temperature. A reduction of around 1400K can be gained if the engine works properly at (φ = 0.2) instead of stoichiometric operation
- The low values of volumetric efficiency seem a serious challenge for the hydrogen engine and further studied are required

ACKNOWLEDGMENTS

The authors would like to express their deep gratitude to Universiti Malaysia Pahang (UMP) for provided the laboratory facilities and financial support.

REFERENCES

COD (College of the Desert), 2001. Hydrogen fuel cell engines and related technologies, module 3: Hydrogen use in internal combustion engines. http://www1.eere.energy.gov/hydrogenandfuelcells/tech_validation/h2_manual.html.

Das, L., R. Gulati and P. Gupta, 2000. A comparative evaluation of the performance characteristics of a spark ignition engine using hydrogen and compressed natural gas as alternative fuels. Int. J. Hydrogen Energy, 25: 783-793.

Das, L., 2002. Hydrogen engine: Research and development programmes in Indian Institute of Technology (IIT), Delhi. Int. J. Hydrogen Energy, 27: 953-965.

Das, L.M., 1990. Fuel induction techniques for a hydrogen operated engine. Int. J. Hydrogen Energy, 15: 833-842.

Furuhama, S. and T. Fukuma, 1986. High output power hydrogen engine with high-pressure fuel injection, hot surface ignition and turbocharging. Int. J. Hydrogen Energy, 11: 399-407.

Ganesh, R.H., V. Subramanian, V. Balasubramanian, J.M. Mallikarjuna, A. Ramesh and R.P. Sharma, 2008. Hydrogen fueled spark ignition engine with electronically controlled manifold injection: An experimental study. Renv. Energy, 33: 1324-1333.

Heywood, J.B., 1988. Internal Combustion Engine Fundamentals. 1st Edn. McGraw-Hill, New York, ISBN: 0-07-028637-X.

Kabat, D.M. and J.W. Heffel, 2002. Durability implications of neat hydrogen under sonic flow conditions on pulse-width modulated injectors. Int. J. Hydrogen Energy, 27: 1093-1102.

Kim Y.Y., T.L. Jong and H.C. Gyeung, 2005. An investigation of the cycle-to-cycle variation in direct injection hydrogen fueled engine. Int. J. Hydrogen Energy, 30: 69-76.

Kim, Y.Y., J.T. Lee and J.A. Caton, 2006. The development of a dual-injection hydrogen-fueled engine with high power and high efficiency, J. Eng. Gas Turbines Power, ASME, 128: 203-212.

Lee, S.J., H.S. Yi and E.S. Kim, 1995. Combustion characteristics of intake port injection type hydrogen fueled engine. Int. J. Hydrogen Energy, 20: 317-322.

Li, H. and G.A. Karim, 2006. Hydrogen fueled spark-ignition engines predictive and experimental performance. J. Eng. Gas Turbines Power ASME, 128: 230-236.

Lynch, F.E., 1983. Parallel induction: A simple fuel control method for hydrogen engines. Int. J. Hydrogen Energy, 8: 721-730.

Nagalingam, B., M. Dübel and K. Schmillen, 1983. Performance of the supercharged spark ignition hydrogen engine. http://www.sae.org/technical/papers/831688.

Pulkrabek, W.W., 2003. Engineering Fundamentals of the Internal Combustion Engines. 2nd Edn., Prentice Hall, New York, ISBN-10: 0131405705.

Rottengruber, H., M. Berckmüller, G. Elsässer, N. Brehm and C. Schwarz, 2004. Direct-injection hydrogen SI-engine operation strategy and power density potentials. http://www.sae.org/technical/papers/2004-01-2927.

Sierens, R. and S. Verhelst, 2001. Experimental study of a hydrogen-fueled engine. J. Eng. Gas Turbines Power ASME, 123: 211-216.

Suwanchotchoung, N., 2003. Performance of a spark ignition dual-fueled engine using split-injection timing. Ph.D Thesis, Vanderbilt University, Mechanical Engineering.

Verhelst, S., R. Sierens and S. Verstraeten, 2006. A critical review of experimental research on hydrogen fueled SI engines. http://www.sae.org/technical/papers/2006-01-0430.

White, C.M., R.R. Steeper and A.E. Lutz, 2006. The hydrogen-fueled internal combustion engine: A technical review. Int. J. Hydrogen Energy, 31: 1292-1305.

Yi, H.S., K. Min and E.S. Kim, 2000. The optimised mixture formation for hydrogen filled. Int. J. Hydrogen Energy, 25: 685-690.